

## Gamma-Ray Spectroscopy Measurements of Fast Ions on ASDEX Upgrade

M. Nocente<sup>1,2</sup>, M. Garcia-Munoz<sup>3</sup>, G. Gorini<sup>1,2</sup>, M. Tardocchi<sup>2</sup>, A. Weller<sup>3</sup>, S. Akaslompolo<sup>4</sup>, R. Bilato<sup>3</sup>, V. Bobkov<sup>3</sup>, C. Cazzaniga<sup>1</sup>, B. Geiger<sup>3</sup>, G. Grosso<sup>2</sup>, A. Herrmann<sup>3</sup>, V. Kiptily<sup>5</sup>, M. Maraschek<sup>3</sup>, R. McDermott<sup>3</sup>, J.M. Noterdaeme<sup>3</sup>, Y. Podoba<sup>3</sup>, G. Tardini<sup>3</sup> and the ASDEX Upgrade Team

<sup>1</sup>*Dipartimento di Fisica “G. Occhialini”, Università degli Studi di Milano-Bicocca, Piazza della Scienza 3, 20126, Milano, Italy*

<sup>2</sup>*Istituto di Fisica del Plasma “Piero Caldirola”, Associazione EURATOM-ENEA-CNR, Via Cozzi 53, 20125, Milano, Italy*

<sup>3</sup>*Max-Planck-Institut für Plasmaphysik, EURATOM Association. Boltzmannstraße 2, D-85748 Garching, Germany*

<sup>4</sup>*Department of Applied Physics, Aalto University School of Science, Association Euratom-Tekes, P.O.Box 14100, FI-00076, Finland*

<sup>5</sup>*JET-EFDA, Culham Science Centre, Abingdon OX14 3DB, United Kingdom*

Electronic mail: [massimo.nocente@mib.infn.it](mailto:massimo.nocente@mib.infn.it)

### Abstract

Evidence of  $\gamma$ -ray emission from fast ions in ASDEX Upgrade (AUG) is presented. The plasma scenarios developed for the experiments involve deuteron or proton acceleration. The observed  $\gamma$ -ray emission level induced by energetic protons is used to determine an effective tail temperature of the proton distribution function that can be compared with Neutral Particle Analyzer measurements. More generally the measured emission rate is used to assess the confinement of protons with energies  $< 400$  keV in discharges affected by Toroidal Alfvén Eigenmode instabilities. The derived information on confined ions is combined with observations made with the AUG Fast Ion Loss Detector.

### 1. Introduction

Gamma-Ray Spectroscopy is being proposed as a diagnostic of confined  $\alpha$ -particles in ITER [1] and used in present-day experiments as a tool to study fast ion physics [2]. In JET, ions in the MeV range produced by Ion Cyclotron Resonance Heating (ICRH) are well confined thanks to the large plasma size and high plasma currents. The recent installation of high resolution spectrometers has enhanced the quality of the  $\gamma$ -ray emission measurements and contributed to the development of nuclear physics based methods and models for the understanding of plasma physics [3,4]. ASDEX Upgrade (AUG) [5] is somewhat smaller than JET in terms of plasma volume and current; however it is well equipped with fast ion diagnostics. These have provided experimental results on the interaction between fast ions and MHD modes, e.g. with the characterization of losses induced by Neoclassical Tearing Modes (NTM), Toroidal Alfvén Eigenmodes (TAE) and Alfvén cascades (AC) [6,7]. The unique possibility to combine information from different diagnostics makes AUG an interesting machine also for  $\gamma$ -ray spectroscopy observations.

The emission of  $\gamma$ -rays from the plasma can be induced on AUG either by fast protons or by fast deuterons interacting with other plasma ions. ICRH at power levels up to 5 MW is available and can in principle be used to push the ions up in energy until they are no longer

TABLE I: Reaction of interest for  $\gamma$ -ray emission studies on AUG

Reactions induced by fast deuterons	Reactions induced by fast protons
$^{14}\text{N}(\text{d},\text{p}\gamma)^{15}\text{N}$ ( $5 \text{ MeV} < E_\gamma < 7 \text{ MeV}$ )	$^{11}\text{B}(\text{p},\gamma)^{12}\text{C}$ ( $9 \text{ MeV} < E_\gamma < 12 \text{ MeV}$ ) $^{10}\text{B}(\text{p},\gamma)^{11}\text{C}$
$^{14}\text{N}(\text{d},\alpha\gamma)^{12}\text{C}$ ( $3 \text{ MeV} < E_\gamma < 5 \text{ MeV}$ )	$\text{d}(\text{p},\gamma)^3\text{He}$ ( $E_\gamma = 5.5 \text{ MeV}$ )

confined by the available plasma current. This paper reports on a series of experiments performed in order to explore the production and confinement of fast ions in AUG using  $\gamma$ -ray spectroscopy in combination with other diagnostics. The paper is organized as follows. Details on the designed scenarios for  $\gamma$ -ray spectroscopy observations on AUG are given in Section 2. Section 3 summarizes the experimental results by comparing observations by  $\gamma$ -ray spectroscopy, Neutral Particle Analyzer (NPA), Fast Ion Loss Detector (FILD) and Mirnov coils. Finally the  $\gamma$ -ray measurements are discussed in more detail in Section 4.

## 2. Plasma Scenarios for $\gamma$ -ray emission

On AUG fast deuterons can induce  $\gamma$ -ray emission through interaction with  $^{14}\text{N}$  impurities. Nitrogen gas is commonly injected into AUG plasmas for divertor cooling; it also has a beneficial effect on energy confinement [8,9]. Several  $\gamma$ -ray emission peaks may be observed with different intensities and characteristic energies in the range  $3 \text{ MeV} < E_\gamma < 7 \text{ MeV}$  (Table I). The latter depend on which particle is produced in the reaction exit channel (mainly  $\alpha$ -particles or protons) and on the excited level of the  $\gamma$ -ray emitting nucleus that is populated. In all cases cross section data available in the literature [10] show a substantial increase for  $E_d > 0.4 \text{ MeV}$ , that can be regarded as an effective threshold deuteron energy for  $\gamma$ -ray emission induced by fast deuterons on  $^{14}\text{N}$ .

Energetic protons can induce  $\gamma$ -ray emission on AUG through capture reactions on either boron or bulk deuterons (Table I). In capture reactions, the  $\gamma$  ray does not result from de-excitation of a heavy nucleus in a two step process (such as  $^{12}\text{C}$  in the  $^{14}\text{N}(\text{d},\alpha\gamma)^{12}\text{C}$  reaction), but is instead the product of a fusion reaction (as for  $\text{d}(\text{p},\gamma)^3\text{He}$ ). Boron is present in the plasma as impurity after machine boronization, which is periodically performed to decrease tungsten accumulation in the plasma core [8]. Deuterium is the major constituent of the bulk plasma. The expected  $\gamma$ -ray peak energies are  $E_\gamma=5.5 \text{ MeV}$  for the  $\text{d}(\text{p},\gamma)^3\text{He}$  reactions and  $9 \text{ MeV} < E_\gamma < 12 \text{ MeV}$  for reactions with boron as target. The main drawback of capture reactions is that the cross section is typically 2 to 3 orders of magnitude lower than that for two step reactions at same energies, with values in the micro-barn range for proton energies of some hundreds of keV (figure 1). On the other hand fast protons are expected to be more easily confined than fast deuterons, as the Larmor radius scales with  $\sqrt{m}$  for ions at the same energy. Full orbit simulations with the GOURDON code [11] for a typical AUG plasma equilibrium with  $B_T=2.5 \text{ T}$  and  $I_p=1 \text{ MA}$  show that the deuteron and proton energies at which first orbit losses become significant are  $E_d \approx 0.8 \text{ MeV}$  and  $E_p \approx 1.5 \text{ MeV}$ , respectively. The acceleration of protons or deuterons requires different heating schemes. As deuterium is the main bulk plasma component, energetic deuterons were created through ICRH tuned to second cyclotron harmonic by exploiting acceleration due to finite Larmor radius effects [12]. The required energetic ion seed was provided by neutral beam injection (energy  $E_d=62 \text{ keV}$ )

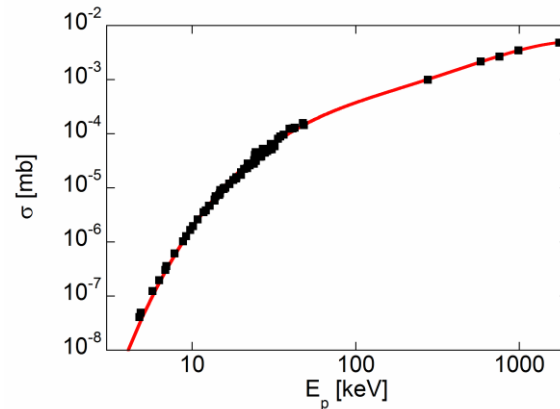


Figure 1. Cross section of the  $d(p, \gamma)^3\text{He}$  reaction as a function of the proton energy in the lab system. Data points are taken from the EXFOR database<sup>1</sup>. The solid line is the best fit to the data using Eq.2.

orthogonal to the magnetic field. Fast protons were instead generated through minority (H)D ICRH heating scheme. Here the ICRH power was coupled to hydrogen ions; these are usually present in AUG deuterium plasmas at a concentration level approaching 5%.

In both scenarios, the plasma bulk density had to be kept as low as possible to facilitate the development of tails in the hundreds keV region. This was particularly challenging for fast deuteron scenarios, where the use of NBI heating determined a density rise, a feature commonly observed in tokamak plasmas. A low density would require a low plasma current but this is in conflict with the need to confine energetic deuterons. Therefore, a trade-off had to be sought for experimentally. Lower densities were more easily achieved in discharges run immediately after machine boronization, thanks to reduced recycling.

A  $\text{LaBr}_3(\text{Ce})$  scintillator designed for high rate operation [13] was used for the observation of  $\gamma$ -rays in discharges with fast protons and deuterons. The detector was placed at a distance of 12 m from the plasma centre, behind a 2 m thick concrete wall. The line of observation was defined by a hole in the concrete wall with a diameter of 8.5 cm, looking through one of the diagnostic ports. A set of polyethylene, lithium and cadmium attenuators was used to reduce neutron induced background on the scintillator, which was found to be significant particularly for discharges with neutral beam injection. Neutron induced background was also the main source of recorded events in the  $\gamma$ -ray energy region  $E_\gamma < 3$  MeV, which forced to put the detector behind the concrete wall. The background event rate was about 20 times lower in the region  $E_\gamma > 3$  MeV.

### 3. Results

#### 3.1. Results from the fast deuteron scenario

Several discharges were performed in order to accelerate deuterons by relying on 2<sup>nd</sup> harmonic ICRH on a perpendicular neutral beam injection providing the required finite Larmor radius, but no  $\gamma$ -ray emission was observed. In all discharges, NPA showed that the fast deuteron energy distribution exceeded the 62 keV NBI injection energy during the superimposed RF heating phase, demonstrating that synergetic NBI+RF heating was indeed taking place. Mirnov coils measurements revealed high frequency MHD activity of the Alfvén type only for few hundred milliseconds in one of the discharges. Few fast ion losses

<sup>1</sup> <http://www-nds.iaea.org/exfor>

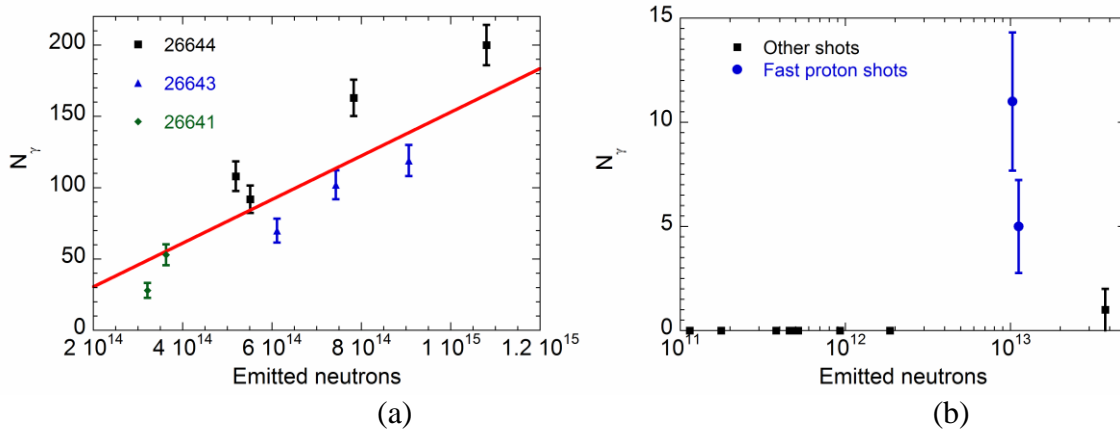


Figure 2. (a) Measured counts in the energy region 9-12 MeV for several AUG discharges and time windows as function of the number of neutrons emitted by the plasma in the same time window. (b) Same as (a), but for discharges with a lower neutron yield. The two discharges in which fast protons were accelerated clearly deviate from the general trend.

induced by MHD activity were correspondingly observed. A key parameter was found to be the electron density, expressed by its core line integrated value  $n_e$ . In most of the discharges  $n_e$  was above  $6 \cdot 10^{19} \text{ m}^{-2}$ , independently of whether the discharge was performed close to boronization or not.

The few observed signatures of fast ion induced MHD activity mentioned above were detected for short time intervals when  $n_e < 6 \cdot 10^{19} \text{ m}^{-2}$ . In these cases, however, magnetic islands also appeared that made the plasma unstable and ultimately led to a disruption.

### 3.2. Results from the fast proton scenario

Two identical discharges (#26615 and #26616) designed for minority heating of protons in (H)D plasmas were performed with  $I_p=1.0 \text{ MA}$  and  $B_T=2.5 \text{ T}$ . Core electron cyclotron resonance heating (ECRH) was used to raise the electron temperature thus decreasing the electron drag on energetic ions. In both discharges  $n_e$  fell in the range  $5\text{-}6 \cdot 10^{19} \text{ m}^{-2}$ . ICRH was applied from 1 s at a total power level of 5 MW for about 1.5 s, with resonance in the plasma centre. A 100 ms NBI blip was used at  $t=2 \text{ s}$  for diagnostic purposes.

A signature of  $\gamma$ -ray emission from  $p+^{11}\text{B}$  and  $p+^{10}\text{B}$  reactions was observed in the measured pulse height spectrum. Figure 2 shows the number  $N_\gamma$  of detected events in the pulse height region 9-12 MeV as function of the absolute neutron emission  $Y_n$  as measured by a combination of neutron yield monitors and activation foils for AUG discharges with different neutron emission levels. A linear scaling between  $N_\gamma=b \cdot Y_n$  with  $b=1.53 \cdot 10^{-13}$  is found for most discharges (Figure 2a). An exception is a set of discharges in which protons were accelerated, where an excess of  $N_\gamma$  events was found. This can be ascribed to the contribution from proton capture on boron. A more clear manifestation of  $\gamma$ -ray emission from fast protons was provided by the observation of the  $E_\gamma=5.5 \text{ MeV}$  peak due to the  $d(p,\gamma)^3\text{He}$  reaction (figure 3). The peak stands out of the background level in a statistically meaningful way.

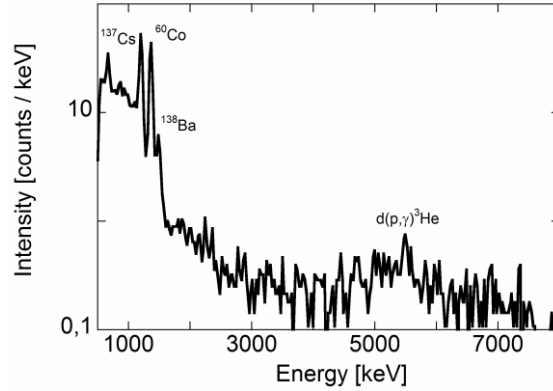


Figure 3. Sum of  $\gamma$ -ray spectra for discharges #26615 and #26616 integrated for 1 s during ICRH. Peaks at low energies are due to energy calibration sources ( $^{137}\text{Cs}$  and  $^{60}\text{Co}$ ) or to the detector intrinsic radioactivity ( $^{138}\text{Ba}$ ). At high energies, the  $E_\gamma=5.5$  MeV peak from the  $d(p,\gamma)^3\text{He}$  reaction is visible above the background level.

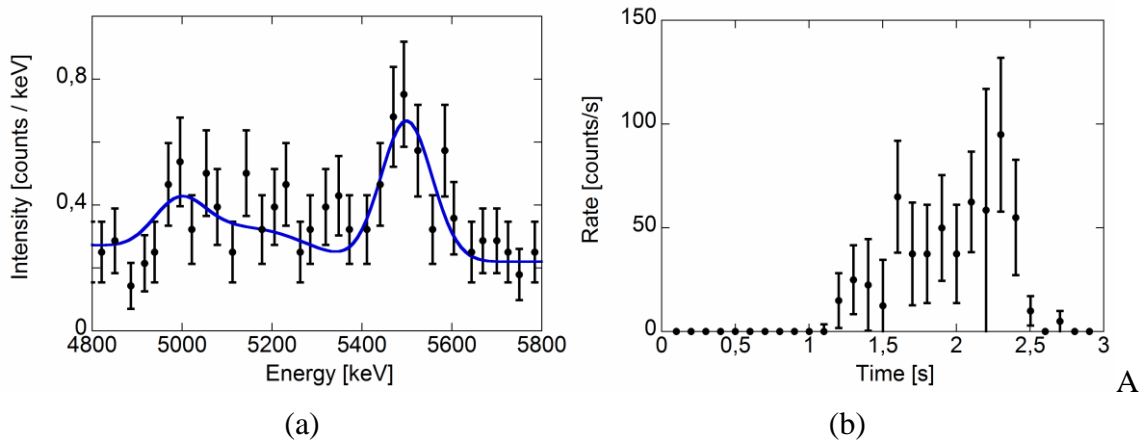


Figure 4. (a) MCNP simulation (full line) of the  $E_\gamma=5.5$  MeV peak from the  $d(p,\gamma)^3\text{He}$  reaction superimposed to data from Figure 3 in the energy range of interest. (b) Time resolved count rate in the  $E_\gamma=5.5$  MeV peak energy range, averaged between the two discharges.

Figure 4 (a) shows the measured  $d(p,\gamma)^3\text{He}$  emission peak. Superimposed to the data is a simulated spectral shape obtained by adding a constant background to the result of a Monte Carlo simulation using the MCNP code (providing the spectrum of energies deposited in the detection crystal) folded with the instrumental energy resolution  $\Delta W_I$  and the expected kinetic broadening  $\Delta W_K$  that results from the relative ion motion as predicted in reference [14] (see below). The simulation describes well the observed features of the peak within the available statistics.

The time resolved count rate under the  $E_\gamma=5.5$  MeV peak, after background subtraction, is shown in figure 4 (b). It is averaged for the two discharges with proton acceleration. The count rate increases with time during radiofrequency heating, with an average value  $M_\gamma=33\pm 6$  counts/s between 1 and 2 s. This value can be used to estimate the temperature of fast protons plasma on the basis of a model calculation of the relation between the plasma  $\gamma$ -ray emissivity and the  $\gamma$ -ray flux yielding the observed detector count rate. To this end the viewing geometry

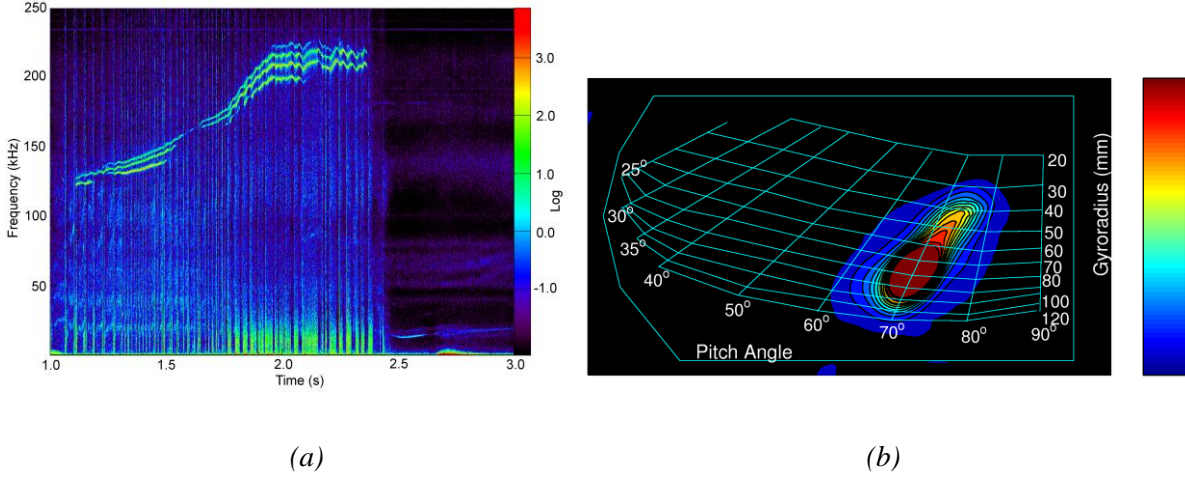


Figure 5. (a) Frequency spectrogram from Mirnov coils showing characteristic frequencies of TAEs driven by fast protons and (b) data from the fast ion loss detector at 1.5 s for discharge # 26615.

of the diagnostics was modeled in terms of an effective plasma volume  $V$  emitting  $\gamma$ -rays within the detector solid angle  $\Omega=A/d^2$  where  $A$  is the detector area exposed to the  $\gamma$ -ray flux and  $d$  its distance from the plasma core. The model assumes isotropic  $\gamma$ -ray emission. The expected signal count rate is then determined from the known full energy peak efficiency  $\eta$  and is  $M_\gamma=\eta S_\gamma V \Omega$ ,  $S_\gamma$  being the  $\gamma$ -ray emissivity. The latter was calculated for a range of proton tail temperatures  $T_p$ . A value of  $T_p=100$  keV provides the best match to the measured rate. We estimate an accuracy of  $\pm 50$  keV in  $T_p$ . This rather large confidence interval results from an estimated error of a factor 2 in the flux calculation, due to neglecting detailed photon transport and systematic uncertainties in the hydrogen concentration value. NPA was also used to measure the tail temperature of fast protons and indicated a temperature of about 70 keV averaged for the two discharges. When combined with  $\gamma$ -ray spectroscopy observations, a  $T_p$  value lying in the range 70-100 keV is inferred. With these values, one can estimate the expected kinematic broadening (FWHM)  $\Delta W_K$  of the  $\gamma$ -ray emission peak due to motion of the reacting ions using equation (5) of reference [14]. The result is  $\Delta W_K \approx 105$ -140 keV that was folded with the instrumental broadening  $\Delta W_I \approx 100$  keV at  $E_\gamma=5.5$  MeV to give the simulated peak shape shown in Figure 4(a). The proton tail temperature could also, alternatively, be derived from the observed  $\gamma$ -ray peak broadening alone, by fitting the measured spectrum for several values of  $\Delta W_K$  and derive the corresponding  $T_p$  according to the model of reference [14], as done in previous works [2]. However, the limited statistics of the measurement and the fact that  $\Delta W_I \approx \Delta W_K$  would not significantly improve the  $T_p$  assessment based on the observed absolute measured rate.

The two plasma discharges with strong proton acceleration were quite rich in terms of fast ion driven MHD activity. Figure 5a shows the frequency spectrogram for shot #26615 detected with Mirnov coils [15] between 1 and 3 seconds (the spectrogram for shot #26616 is very similar and is not shown). Frequencies due to Toroidal Alfvén Eigenmodes (TAE) driven by energetic protons appear in the range 100-250 kHz, from 1.11 s. The toroidal mode numbers, obtained by measurements of the phase shifts among coils displaced at different toroidal

locations, are  $n=3-6$  between 1 and 2 s; TAEs with lower toroidal numbers were also excited after the NBI blip at 2 s. A complex loss pattern in phase space was correspondingly detected with FILD [16] (figure 5b). Prompt losses with pitch angles in the range  $70-75^\circ$  and Larmor radii between 80-100 mm were observed at  $t=1.06$  s, i.e. in coincidence with ICRH and 50 ms before MHD was detected on the magnetic coils. These are interpreted as first orbit losses of ions with energies  $> 1.5$  MeV that were produced by ICRH on unconfined trajectories. At later instants, few ms after the appearance of TAEs in the magnetics, a second bright spot corresponding to energies in the range 550-800 keV was observed, soon extending to higher energies up to about 2 MeV and lasting until the end of the heating phase. TAEs also significantly enhanced losses in the pitch angle/Larmor radius region corresponding to protons accelerated by ICRH on unconfined orbits observed at  $t=1.06$  s. No losses of protons with energies  $< 400$  keV were observed throughout the discharges.

#### 4. Discussion

The observed  $\gamma$ -ray reactivity from the  $d(p,\gamma)^3\text{He}$  reaction can be interpreted as follows. For protons that are much faster than the target deuterons, the reactivity  $Y_\gamma$  is given by

$$Y_\gamma = \int y_\gamma(E_p) dE_p \quad (1)$$

where the integrand  $y_\gamma(E_p)=f(E_p)v\sigma(E_p)$  is the differential reactivity and expresses the  $\gamma$ -ray emission intensity as function of the proton energy  $E_p$  [4]. Here  $f$  represents the proton energy distribution,  $v$  its velocity and  $\sigma$  the reaction cross section. The latter was parameterized here as [17,18]

$$\sigma(E_p) = \frac{S(E_p)}{E_p} \exp(-\beta_G / \sqrt{E_p}) \quad (2)$$

where  $S(E_p)$  is the astrophysical factor and  $\beta_G$  the Gamow constant. Cross section data of the  $d(p,\gamma)^3\text{He}$  reaction in the proton energy range 10 keV-2 MeV can be described (figure 1, solid line) with equation (2) by expressing  $S(E_p)$  as a fourth order polynomial [19,20]

$$S(E_p) = A_0 + A_1 \cdot E_p + A_2 \cdot E_p^2 + A_3 \cdot E_p^3 + A_4 \cdot E_p^4 \quad (3)$$

with best fit parameter values as given in Table 2.

The cross section parameterization is used to calculate the differential reactivity  $y_\gamma(E_p)$  for several tail temperatures of the fast proton energy distribution (figure 6). For tail temperatures in the range 70-100 keV, most of  $\gamma$ -ray emission involves protons with  $E_p < 400$  keV, with a peak energy (the so called "Gamow peak energy"  $E_{Gp}$ ) between 120 keV and 180 keV. This result, combined with the observation that the  $\gamma$ -ray emission rate increases with time even though TAE fluctuations appear in the magnetic traces, suggests that protons with  $E_p < 400$  keV are well confined and not significantly affected by TAEs. This is also in agreement with the lack of losses for  $E_p < 400$  keV observed with the FILD.

TABLE II: Gamow constant and fit parameters for the astrophysical factor  $S(E_p)$ .  $E_p$  is expressed in MeV

$\beta_G$	1.07	$A_2$	1.21E-2
$A_0$	8.09E-4	$A_3$	-5.26E-3
$A_1$	1.92E-3	$A_4$	6.52E-4

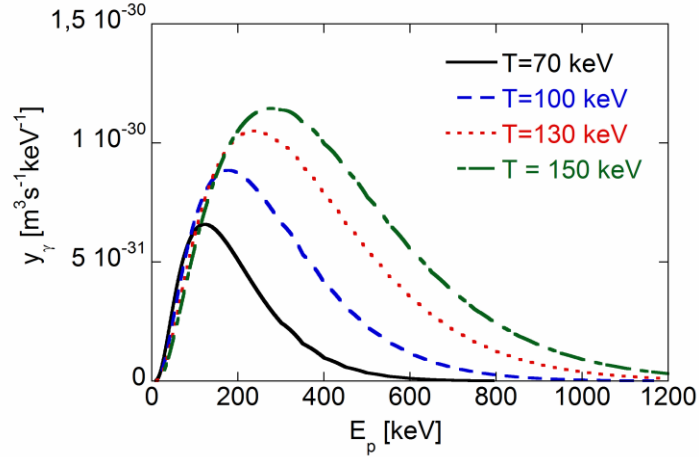


Figure 6. Differential reactivity of the  $d(p, \gamma)^3\text{He}$  reaction calculated for different tail temperatures as function of proton energy.

Further insight is obtained by calculating resonance curves in phase space between fast protons with their turning points at the radial location of the magnetic axis and TAEs with toroidal mode numbers  $n=3-6$  as observed between 1 and 2 s with Mirnov coils. A necessary (but not sufficient) condition for particle-mode resonance is that the relation  $n\omega_\phi - p\omega_\theta - \omega \approx 0$  is satisfied. Here  $\omega$  and  $n$  are the measured frequency and toroidal number of the mode,  $\omega_\phi$  and  $\omega_\theta$  the toroidal precession and poloidal transit frequency of the resonating ion,  $p$  the bounce harmonic [21]. Figure 7 shows contour plots of the function  $\log(1/|n\omega_\phi - p\omega_\theta - \omega|)$  for  $n=3-6$  and  $p=-3$  to 3 in the  $(E, z)$  plane (which is equivalent to the  $(E, p_\phi)$  plane for ICRH ions with turning points at the radial location of the magnetic axis [7];  $p_\phi$  indicates the toroidal component of the canonical angular momentum). The curves were obtained from the results on  $\omega_\phi$  and  $\omega_\theta$  calculated with the GOURDON code [11] using the magnetic equilibrium at  $t=1.5$  s. Two observations can be made. The first is that virtually all energies may resonate with the observed TAEs, as was found in another AUG discharge with different  $I_p$  and  $B_T$  values [7]. This also explains why losses in a quite wide energy range were observed on the FILD. The second observation is that protons in the energy range  $E_p < 400$  keV can resonate with the TAEs only through negative bounce harmonics. The latter, combined with the observed monotonic  $\gamma$ -ray emission rate, suggests that mode resonances involving negative bounce harmonics do not significantly affect fast ion confinement on AUG, in agreement with the absence of losses for  $E_p < 400$  keV as detected by the FILD. As a final consideration, it would be highly desirable to have a better overlap between the region where losses were

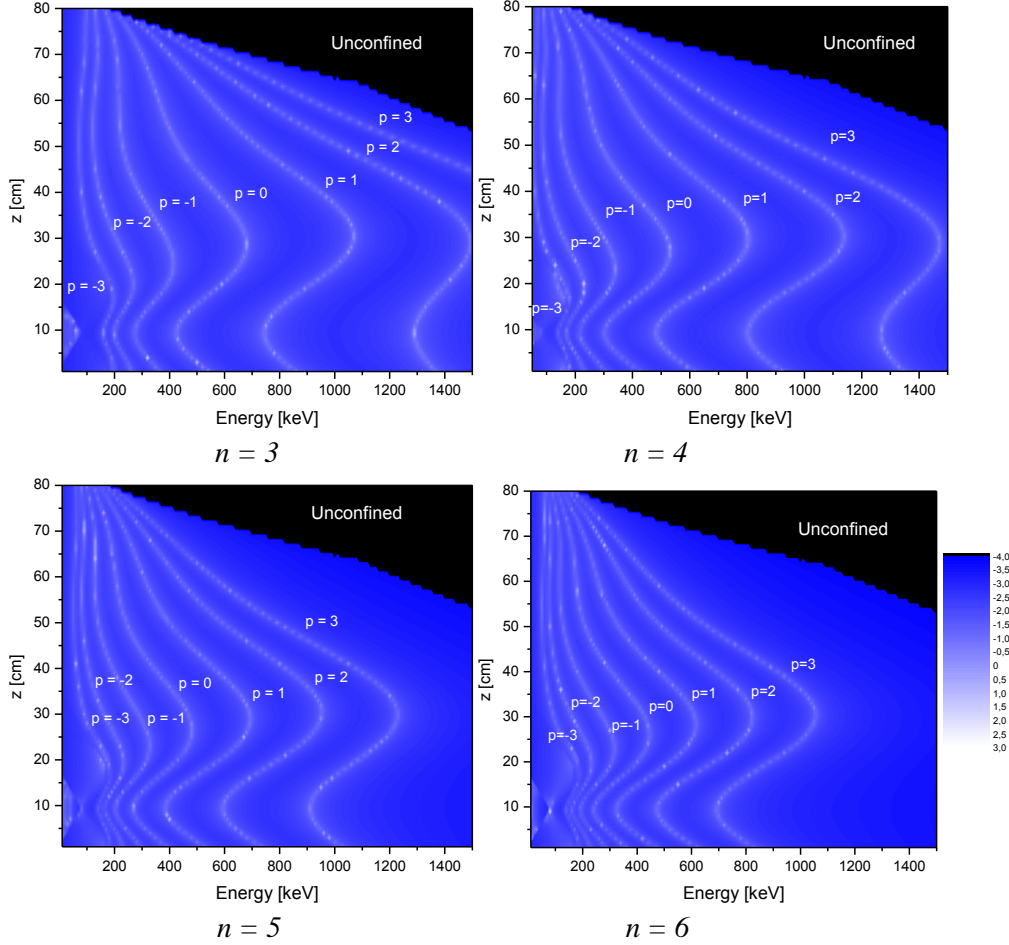


Figure 7. Calculated resonances in phase space between protons having their turning points on the magnetic axis and TAEs with toroidal mode numbers  $n = 3$  to 6. Only curves for bounce harmonics  $p = -3$  to 3 are shown.

observed and that responsible for  $\gamma$ -ray emission in future experiments on AUG. This can be done by increasing the Gamow peak energy. A simplified analytic derivation, in which the energy dependence of the astrophysical factor  $S(E)$  is neglected, shows that  $E_{Gp}$  scales as  $T_p^{2/3}$  [17]. A Gamow peak energy of about 400 keV would of course provide almost complete overlapping but is beyond what can be reasonably achieved on AUG with the present machine parameters and power levels. More realistically one could try to reduce the electron density down to  $3\text{-}4 \cdot 10^{19} \text{ m}^{-2}$  by fast current ramp up; combined with improvements of at least 10% in the RF coupling, this would yield proton tail temperatures  $T_p \approx 150$  keV, based on Stix scaling of the tail temperature on  $n_e$  and RF power [12]. As shown in figure 6, the Gamow peak energy is  $E_{Gp} = 280$  keV at  $T_p = 150$  keV and about 40% of the  $\gamma$ -ray reactivity is due to protons with  $E_p > 400$  keV. Furthermore the  $\gamma$ -ray reactivity scales roughly as  $T_p$  in the range  $T_p = 50\text{-}200$  keV meaning that improvements in measurement statistics are to be expected, possibly allowing for quantitative comparison with diagnostic information on lost protons from the FILD.

## 5. Conclusion

First measurements of  $\gamma$ -ray emission due to fast ions in ASDEX Upgrade were performed. Emission from proton capture reactions on boron and deuterium was observed in two (H)D discharges with radiofrequency heating in the minority acceleration scheme. The observed count rate was used to infer the values of the fast proton tail temperature. A value in the range 70-100 keV is compatible with both  $\gamma$ -ray and NPA observations. TAE fluctuations were observed with Mirnov coils throughout the heating phase and associated proton losses were detected with the FILD. The observed emission rate, combined with calculations of the  $\gamma$ -ray differential reactivity and particle-mode resonance curves in phase space, revealed that resonances with negative values of the bounce harmonics did not significantly affect fast ion confinement ( $E_p < 400$  keV). Future  $\gamma$ -ray spectroscopy measurements of confined protons in AUG should be aimed at raising the proton tail temperature up to 150 keV and above, where the improved measurement statistics would allow for even better comparison with diagnostic information on lost protons from the FILD.

## 6. Acknowledgment

This work was supported by EURATOM and carried out within the framework of the European Fusion Development Agreement. The views and opinions expressed herein do not necessarily reflect those of the European Commission. The computing resources of CSC - IT centre for science were used in the data-analysis.

## References

- [1] KIPTILY, V. G., CECIL, F. E. and MEDLEY S. S., "Gamma ray diagnostics of high temperature magnetically confined fusion plasmas", *Plasma Phys. Control. Fusion* **48** (2006) R59
- [2] KIPTILY V.G et al., " $\gamma$ -ray diagnostics of energetic ions in JET", *Nucl. Fusion* **42** (2002) 999
- [3] TARDOCCHI M. et al., "Spectral broadening of characteristic  $\gamma$ -ray emission peaks from  $^{12}\text{C}(^3\text{He},\text{p})^{14}\text{N}$  reactions in fusion plasmas", submitted to *Phys. Rev. Letters*
- [4] PROVERBIO I., NOCENTE M., KIPTILY V. G., TARDOCCHI M. and GORINI G., "The  $^{12}\text{C}(^3\text{He},\text{p})^{14}\text{N}$  reaction cross section for  $\gamma$ -ray spectroscopy simulation of fusion plasmas", *Rev. Sci. Instrum.* **81** (2010) 10D320
- [5] ZOHN H. et al., "Overview of ASDEX Upgrade Results", *Nucl. Fusion* **49** (2009) 104009
- [6] GARCIA-MUNOZ M. et al. "Convective and Diffusive Energetic Particle Losses Induced by Shear Alfvén Waves in the ASDEX Upgrade Tokamak", *Phys. Rev. Letters* **104** (2010) 185002
- [7] GARCIA-MUNOZ M. et al., "MHD induced fast-ion losses on ASDEX Upgrade", *Nucl. Fusion* **49** (2009) 085014
- [8] GRUBER O. et al., "Compatibility of ITER scenarios with full tungsten wall in ASDEX Upgrade", *Nucl. Fusion* **49** (2009) 11501
- [9] TARDINI G. et al., "Core transport and pedestal characteristics of nitrogen seeded H-mode discharges in ASDEX Upgrade", *Proc. 37th EPS Conference on Plasma Physics* (2010), P1.1097

- [10] PELLEGRINO S., BECK L. and TROUSLARD P., "Differential cross sections for nuclear reactions  $^{14}\text{N}(\text{d},\text{p}_5)^{15}\text{N}$ ,  $^{14}\text{N}(\text{d},\text{p}_0)^{15}\text{N}$ ,  $^{14}\text{N}(\text{d},\alpha_0)^{12}\text{C}$  and  $^{14}\text{N}(\text{d},\alpha_1)^{12}\text{C}$ ", Nucl. Instrum. Meth. B (2004) 140-144
- [11] GOURDON C., "Programme Optimise de Calculs Numeriques dans les Configurations Magnetiques", Centre d'etudes nucleaires de Fontenay aux Roses (1970)
- [12] STIX T.H., "Waves in Plasmas", Ed. Springer (1992)
- [13] NOCENTE M. et al., "Energy resolution of gamma-ray spectroscopy of JET plasmas with a  $\text{LaBr}_3$  scintillator detector and digital data acquisition", Rev. Sci. Instrum **81** (2010) 10D321
- [14] CECIL F.E. and NEWMAN D.E., "Diagnostics of high temperatures deuterium and tritium plasmas by spectrometry of radiative capture reactions", Nucl. Instrum. Methods **221** (1984) 449
- [15] ZOHRM H. et al., "MHD stability and disruption physics in ASDEX Upgrade", Plasma Phys. Control. Fusion **37** (1995) A313
- [16] GARCIA-MUNOZ M., FAHRBACH H.U. and ZOHRM H., "Scintillator based detector for fast-ion losses induced by magnetohydrodynamic instabilities in the ASDEX upgrade tokamak", Rev. Sci. Instrum. **80** (2009) 053503
- [17] GAMOV G., Z. Phys. 51 (1928) 204
- [18] BURBIDGE E.M. et al., Rev. Mod. Phys. 29 (1957) 547
- [19] BOSCH H.S. and HALE G.M., "Improved formulas for cross-sections and thermal reactivities", Nucl. Fusion **32** (1992) 611
- [20] NOCENTE M., GORINI G., KALLNE J. and TARDOCCHI M., "Cross section of the  $\text{d} + {}^3\text{He} \rightarrow \alpha + \text{p}$  reaction of relevance for fusion plasma applications", Nucl. Fusion **50** (2010), 055001
- [21] HEIDBRINK W.W., "Basic physics of Alfvén instabilities driven by energetic particles in toroidally confined plasmas", Phys. Plasmas **15** (2008) 055501